International Journal of Fluid Machinery and Systems
Vol. 3, No. 2, April-June 2010

Original Paper

Computational Study of Magnetically Suspended Centrifugal Blood Pump (The First Report: Main Flow and Gap Flow)

Yoshifumi Ogami[1], Daisuke Matsuoka[2] and Masaaki Horie[3]

[1]Department of Mechanical Engineering, Ritsumeikan University
1-1-1 Noji-Higashi, Kusatsu, 525-8577, Japan, y_ogami@cfd.ritsumei.ac.jp
[2] Department of Mechanical Engineering, Ritsumeikan University
[3]Department of Mechanical Engineering, Setsunan University
17-8 Ikedanakamachi, Neyagawa, Osaka, 572-8508, Japan, m-horie@mec.setsunan.ac.jp

Abstract

Artificial heart pumps have attracted the attention of researchers around the world as an alternative to the organ used in cardiac transplantation. Conventional centrifugal pumps are no longer considered suitable for long-term application because of the possibility of occurrence of blood leakage and thrombus formation around the shaft seal. To overcome this problem posed by the shaft seal in conventional centrifugal pumps, the magnetically suspended centrifugal pump has been developed; this is a sealless rotor pump, which can provide contact-free rotation of the impeller without leading to material wear. In Europe, clinical trials of this pump have been successfully performed, and these pumps are commercially available. One of the aims of our study is to numerically examine the internal flow and the effect of leakage flow through the gap between the impeller and the pump casing on the performance of the pump. The results show that the pressure head increases compared with the pump without a gap for all flow rates because of the leakage of the fluid through the gap. It was observed that the leakage flow rate in the pump is sufficiently large; further, no stagnant fluid or dead flow regions were observed in the pump. Therefore, the present pump can efficiently enhance the washout effect.

Keywords: Artificial Heart, Blood Pump, Computational Fluid Dynamics, Internal Flow, Turbomachinery

1. Introduction

A long-lasting artificial heart has been drawing attention from the world as a therapeutic device which can replace a cardiac transplantation. Various types of artificial hearts have been researched/developed in the U.S. and Europe, and approved for the use in the medical practice after clinical studies (Kyo et al. [1]). These artificial hearts have been used as a bridge to the cardiac transplantation (Bridge to Transplant: BTR), a treatment to induce recovery of the patient's heart (Bridge to Recovery: BTR) and as a permanent use of a ventricular assist system (Destination Therapy: DT) (Matsumiya [2]). It is thought that the artificial hearts, which can be used permanently will be more available in Japan as well in the future since the number of donors is too small for the number of patients who require cardiac transplantation. Meanwhile, the Ministry of Health and Welfare has been accelerating approvals of some artificial hearts including the magnetically suspended centrifugal blood pump (Ono [3]), the subject of this study, and the practical use of these next-generation artificial hearts has been highly expected.

The use of a traditional turbo blood pump had been limited for a few days since the axial seal inside the casing is likely to induce hemolysis (destruction of blood cells) or thrombosis formation due to frictional heat, and contamination by foreign substances or blood leakage may occur at the seal. In the past, the precessional centrifugal blood pump (Akamatsu [4], [5]) was once introduced as a device which had resolved the problem regarding the axial seal. However, a long-term use was not possible with this pump since its diaphragm was durable only for about 2 weeks. Therefore, Akamatsu et al. developed the magnetically suspended centrifugal blood pump (Akamatsu [4]-[6], Tsukiya and Akamatsu [7]) in collaboration with NTN Corporation in order to resolve the problem mentioned earlier. This system was produced by Terumo Corporation and approved for marketing (received the CE mark) in E.U. in February, 2007 (Terumo Heart Inc. [8]) based on excellent results of clinical studies conducted in Germany, Austria and France.

Received January 26 2010; accepted for publication March 27 2010: Review conducted by Prof. Wang Leqing. (Paper number O10002)
Corresponding author: Yoshifumi Ogami, Professor, ogami@se.ritsumei.ac.jp

In order to prevent hemolysis or thrombosis formation, the magnetically suspended centrifugal blood pump is designed in the way that the impeller can rotate in the blood without any contact inside the casing by the permanent magnet and the electromagnet (Akamatsu [7]); hence, it does not have a rotation axis. Therefore, there is a gap between the impeller and the casing. According to the structure, this pump is classified as a low specific speed and low Reynolds number pump; the studies regarding such pumps conducted by Kurokawa et al. [9], [10] and Matsui et al. [11] may be interesting. Chua et al. [12], [13] performed a numerical simulation of the internal flow when the shape of the blade was different from that of this pump, and reported that the internal flow changed according to the position of the blade due to the different velocity or pressure distribution and that the amount of flow which went through the gap corresponded to about 20% of the flow expelled by the impeller. However, there is no report which explains how the gap flow, which is characteristic to this pump, affects the entire pump system.

In this study, we created a calculation model which reproduced the gap between the impeller and the casing, and another model assuming that there is no gap. Then, we performed a numerical simulation to clarify the effect of the gap flow on the entire pump, including the main flow and the characteristics of the pump. As a result, it was confirmed that the gap could give the following advantages with such a special pump system, although it is usually considered undesirable as the leakage flow results in decreased efficiency.

1. Increased pressure being produced
2. The main flow with less loss
3. "Wash-out" effect to prevent thrombosis formation

Further details are reported in this study. The unit of pressure was determined to be mmHg, in addition to Pa, as this pump is used in the medical settings.

2. Numerical Analysis Method

2.1 Magnetically Suspended Centrifugal Blood Pump

As mentioned earlier, the impeller is rotating while being suspended in the blood without any contact inside the casing by the magnetic force in this blood pump. Hence, in order to improve the stability in the blood, radial straight blades with 90 degree-angle at the inlet and outlet and a double volute are used for the impeller in this system (Akamatsu [5]). Specifications of this blood pump are as follows: generated pressure P=100-120 mmHg, output Q=5 L/min, number of impeller rotations n=2000 min^{-1}, specific velocity = approximately 100, and mechanical Reynolds number R_e=5.0×10^4, approximately; the specific velocity and Reynolds number are low for a turbo machine. In this blood pump, the required height of the blade, b, is also less than 1.0 mm according to the ordinary design. However, it is predicted that adequate pumping effects cannot be achieved with this size due to the effect of the boundary layer inside the impeller. Hence, in order to secure the sufficient flow path, the height of the blade, b, has been determined as 3.5 mm in this pump. As the impeller is magnetically suspended in the blood and rotating without any contact inside the casing, there is a 0.25 mm gap between the impeller and casing. Moreover, as this is an implantable cardiac assistive blood pump, the diameter of the pump inlet and outlet must be about 10 mm, considering the relationships with a cannula, which is used when implanting the device, and aorta. It should be noted that there is some restriction with this blood pump as described above due to the problems regarding the conditions of use.

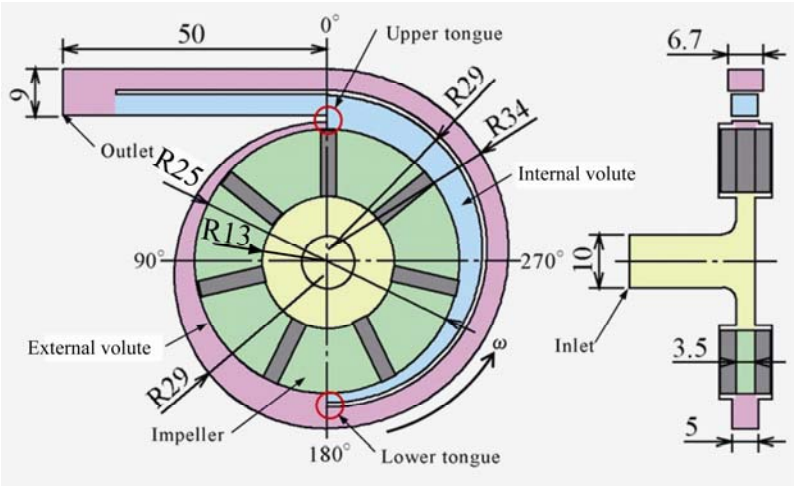

Fig. 1 Model for simulation

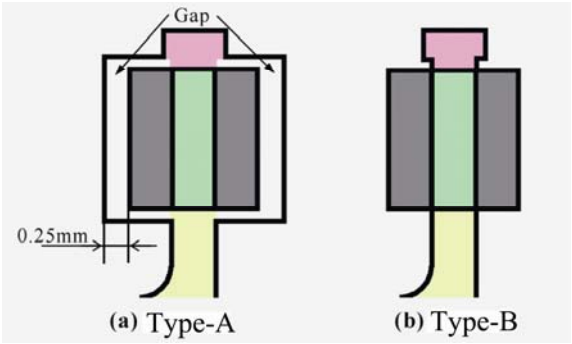

Fig. 2 Schema of gap section

2.2 Numerical Analysis Model

A general-purpose thermal fluid analysis software, "FLUENT", produced by ANSYS, Inc. was used in this study. The numerical analysis was performed with the finite volume method; conservation equations for mass and momentum were integrated at each control volume, and then the discretized equations were resolved. As the mechanical Reynolds number R_e is about 5.0×10^4 in this study, the k-ω model, which is appropriate for the complex flow with separation, was used for the turbulence model (Ansys Inc. [14]). The "QUICK" method was used for the difference schemes of the equations of motion, turbulent energy, and the dissipation rate, and "SIMPLE" method was for the analyses of pressure / velocity (Ferziger [15]).

The computation model is shown in Fig.1. This pump consists of the inlet, impeller, volute and gap. For the impeller, the radial straight blades were also used in the computation as follows: number of blades Z_I =7, height of the blade b=3.5 mm, internal circumference r_1=13 mm, and external circumference r_2=25 mm. The actual pump has a slight taper at the inlet to change the axial flow to radial, and the rectangular section at the volute is changed to circular at the outlet. However, instead of using such a complex-shaped system, we have designed a pump which has a flat wall at the inlet and a rectangular section at the pump outlet with the area size similar to that of the actual pump as the purpose of this study is to clarify qualitative nature of the pump. The rest of the shape is the same, and even the gap between the impeller and casing (Gap in Fig.2), S_L =0.25 mm, is precisely reproduced. Hereinafter, the analytical model with the gap is referred to as type-A. In addition, for the sake of a comparison, a system without the gap is also created by altering type-A as another analytical model without a gap flow. This model is referred to as type-B.

The computational grid of each computational model is all structural, and the numbers of grids in the type-A model with the gap and type-B model without the gap are 234,184 and 116,452, respectively. The grid dependency was studied using analytical models with which the number of grids was nearly the half and double of type-A. As there was little difference in generated pressure and flow patterns at the quasi-steady time, the models with the abovementioned numbers were used for the sake of saving time for computation. Furthermore, the tongues located at θ=0°and θ=180°in Fig.1 are defined as upper tongue and lower tongue, respectively, and the volutes originated from these tongues are defined as external volute and internal volute, respectively.

2.3 Analytical conditions

The total pressure was set as 0 at the inlet, and analyses were made under 7 conditions with the outlet flow ranged from Q=0.0 L/min to 10.0 L/min. The working fluid was assumed to be blood, but the property values of blood varies before and after exercise or according to the health conditions; the specific gravity is about 1.05-1.06, and the viscosity is about 3-4 times higher than water. In this report, density was set as ρ_B= 1056 kg/m^3, and viscosity coefficient was set as μ_B=3.5×10^{-3} Pa· s. In addition, the number of impeller rotation was set as n=2000 min^{-1}. The rotating standard reference frame was defined for the impeller, and the sliding mesh method was used at the border of the rotating part and the still part. As it is unsteady computation, time interval was set as Δt=1.0×10^{-4} s considering the stability conditions.

Thereafter, in the results of further computation, the mean values of one rotation from the 5th to the 6th rotation, where quasi steady state was achieved, were obtained for the pressure (P, P_{TL}) and the amount of flow (Q, Q_L and Q_I), and instantaneous values were obtained for velocity, pressure and vorticity distribution at the 6th rotation.

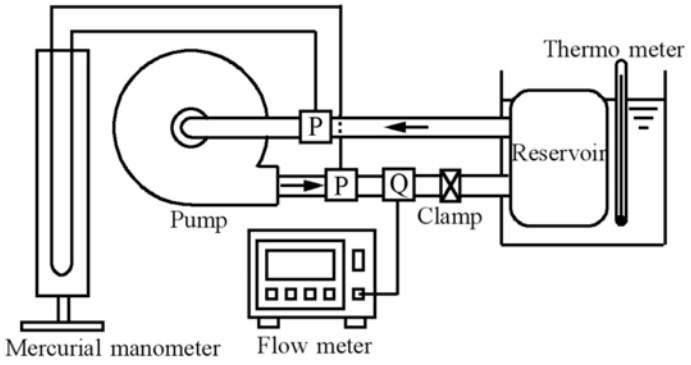

Fig. 3 Schema of experimental circuit

3. Characteristics of the Pump

In order to verify reliability of the results obtained from the numerical simulation, these values were compared with actual measurement values. The overview of the experimental device is shown in Fig.3. The glycerin solution kept at 37ºC (density ρ_G=1120 kg/m^3 and viscosity coefficient μ_G=3.8×10^{-3} Pa·s) was used as the working fluid, and the number of impeller rotation was set as n=2000 min^{-1}. The output, Q=0.0-10.0 L/min, was adjusted by an aperture at every 0.5 L/min, and generated pressure was measured by the mercurial manometer at each amount of flow.

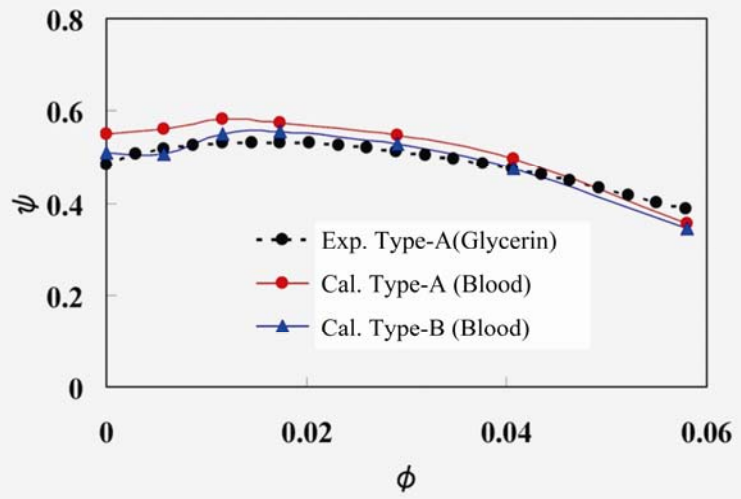

Fig. 4 Pump characteristics

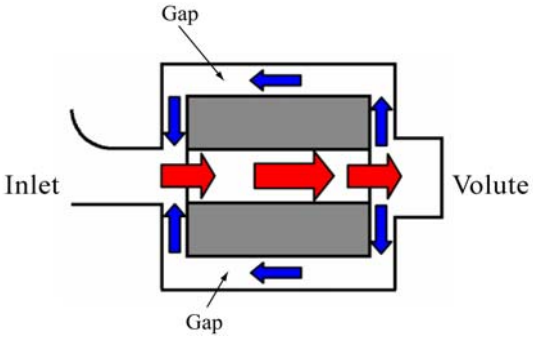

Fig. 5 Schema of flow pattern in gap

The characteristics of the pump obtained from the experiment and simulation are shown in Fig.4. The abscissa and ordinate indicate non-dimensional flow ϕ and non-dimensional pressure ψ, respectively. The normal adult output, Q≈5.0 L/min, approximately, is equivalent to ϕ =0.03, and the blood pressure P≈120 mmHg, approximately, is equivalent to ψ =0.55. The measured values (marked with black circles) and the computation results of type-A analysis model with gap (marked with red circles) reveal that the non-dimensional pressure ψ slightly increases along with the increase of non-dimensional flow ϕ. It reaches the maximum around ϕ =0.015, but thereafter decreases steadily. The simulation results generally correspond to the actual experimental results, although the analytical values are somewhat larger than the measured values within this computational range except when the amount of flow is large.

The computation results for type-A with a gap (marked with red circles) and type-B without a gap (marked with blue triangles) reveal that the generated pressure is larger in type-A than in type-B. This will be further discussed in the following chapters. When there is a gap as shown in Fig.5, the fluid energized by the impeller rotation flows backward from the volute to the inlet through the gap, and then re-enters the impeller. Therefore, the amount of flow going through the impeller increases by the amount of gap flow which flows back, compared to the amount of outlet flow. Therefore, it can be thought that the generated pressure is greater with a gap due to the increased amount of the internal flow of the impeller compared to the system without the gap (See the following Chapter 5and 7).

4. Internal Flow of the Impeller

The followings are described in Fig.6: (a) velocity distribution, (b) pressure distribution, (c) vorticity distribution of the internal flow of the impeller at Q=5.0 L/min of type-A and (d) velocity distribution of the internal flow of the impeller at Q=5.0 L/min of type-B. In Figures 6 (a) and (d), absolute velocity is described at the inlet and volute, and relative velocity is described at impeller, taking the rotation into consideration. The flow patterns are shown with the thick arrows and the letters. The blade closest to the upper tongue is marked 1, and the numbering continues counterclockwise. The flow from the inlet to the volute inside the impeller is referred to as the forward current, and the flow from the volute to the inlet is referred to as the backward current. In vorticity distribution of Fig.6 (c), the positive values in the concentration map indicate the counterclockwise vorticity and the negative values indicate the clockwise vorticity. The black line in the figure represents equivorticity where the vorticity becomes zero. All of these figures show the central section in the direction of the height of the blade.

The velocity distribution of Fig.6 (a) shows that the forward current and backward current develop inside the impeller, and the flow condition varies in between all blades depending on each position. This occurs since the flow path is broader than necessary with the height of the blade b (3.5 mm), which is larger than that of the ordinary design, and the inlet and outlet angles of the blades are 90°. In the deeper observation, the forward current develops in the broad area by the pump action in between 1 and 2, but due to the effect of the clockwise vortex (around "a") which developed when the blade passed the upper tongue, the flow no longer goes along the blade but leaves from the anterior surface of the blade around the tip (b→ b'). In between 2-3, the vortex (a) which used to be present at the tip of the blade between 1 and 2 flows out to the volute, and the forward current starts flowing along the anterior surface of the blade (c→ c'). Furthermore, on the posterior surface of the blade 3, the forward current induces development of a counterclockwise vortex (d). In between 3-4, as seen in the pressure distribution in Fig.6 (b), the pressure at the volute increases as the volute area increases. As it becomes more difficult to flow toward the volute, the area where the forward current develops becomes smaller (e→ e'); therefore, it becomes more likely that the forward current develops only on the anterior surface of the blade. The vortex (d) in between 2-3 grows into another vortex (f), which is even larger, in between 3-4. Since then, the backward current starts to develop from the volute to the impeller. The backward current develops more

prominently in between 4-5 than in between other blades (g→ g'). This occurs since the increased pressure at the volute induces the backward current of the fluid, which cannot flow out to the volute side, to the impeller side where the pressure is low. The vortex (h) is thought to develop when the part of the fluid, which has flowed backward, is flowing toward the internal volute side starting from the lower tongue. The internal flow of the impeller on the internal volute side of 5-1 is axially symmetrical to that on the external volute side. Further explanations are not provided here since the tendency of the flow is similar to that developed in between 1-5 blades.

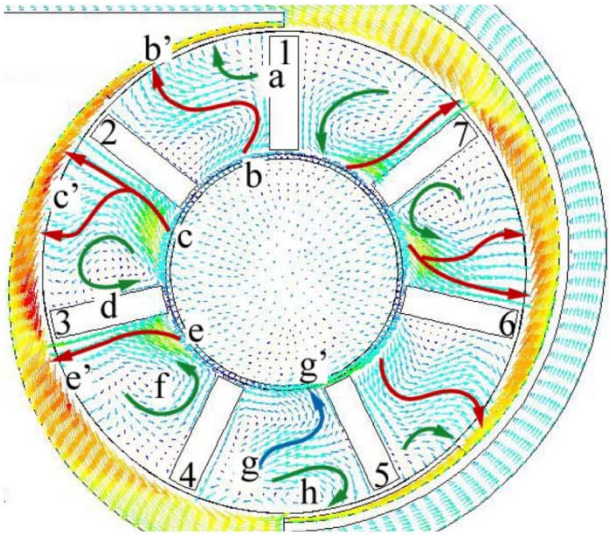

(a) Velocity dstribution of Type-A

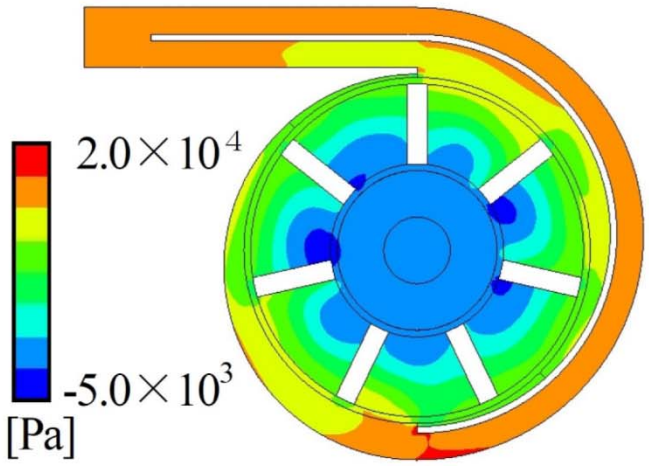

(b) Pressure dstribution of Type-A

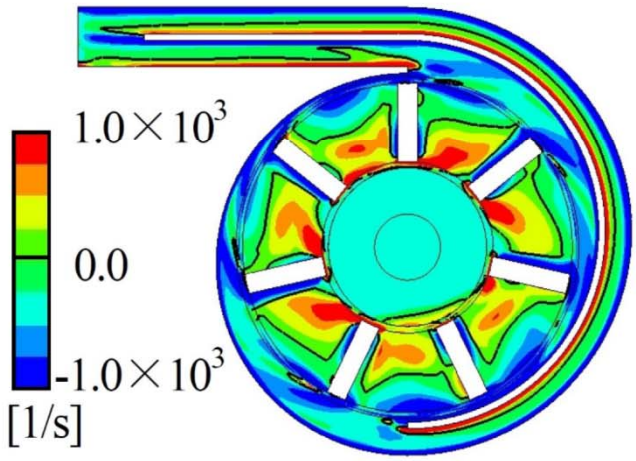

(c) Vorticity dstribution of Type-A

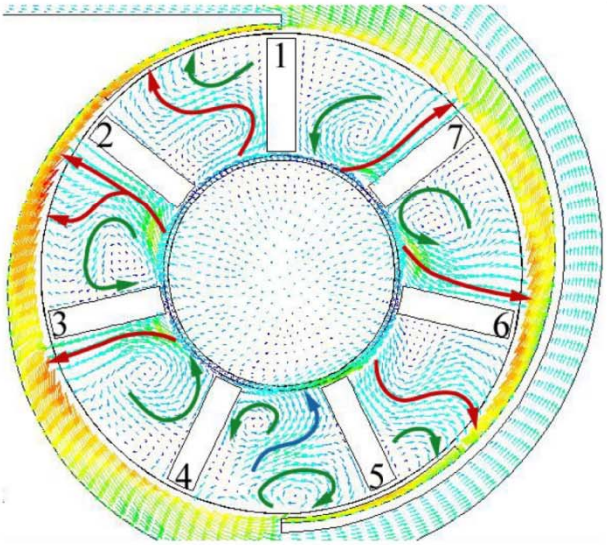

(d) Velocity dstribution of Type-B

Fig. 6 Internal flow at main section

The pressure distribution in Fig.6 (b) shows that higher pressure is observed in the area where the forward current develops along the anterior surface of the blades (2, 3 and 6) compared to the area on the anterior surface of the other blades. On the other hand, the pressure is low in the area where the flow stops or a vortex develops (around the inlet on the posterior surface of the blades 2, 3, 6, and 7). Furthermore, the condition of the internal flow of impeller can be more clarified by studying not only the velocity distribution but also the vorticity distribution presented in Fig.6 (c). The vorticity distribution suggests that the forward current and backward current pass around the equivorticity line where the vorticity is 0, and the former current flows toward the volute and the latter the inlet, respectively. The comparison of velocity distributions between (a) and (d) of Fig.6 reveals that the area where the forward current develops is greater in type-A, which has a gap, than type-B, with no gap. This is because both forward and backward currents develop only inside the impeller in type-B since there is no gap, while in type-A backward current develops in the gap from the volute toward the inlet, and therefore the amount of backflow which goes through the impeller is reduced. Further details are shown in the following chapter.

The amount of flow at Q=5.0 L/min in between each blade around the periphery of the impeller and the amount of outflow from the impeller Q_I are shown in Table 1. This value is the mean amount of flow in between each blade when the blades rotate by 1 pitch from the position shown in Fig.6, while Q_I is the mean amount of flow around the entire impeller outlet. The positive value indicates a forward current, and the negative value indicates a backward current. The findings suggest that the amount of the forward current increases after the tongue and decreases as it approaches toward the tongue in both type-A and type-B. A negative value is reported in between 3-4 in type-B, suggesting that a certain amount of backward current has been equally developed. The value of Q_I in type-A, which has a gap, is 7.1 L/min, exceeding the value of the outlet flow Q. This occurs because the flow inside the gap from the volute to the inlet (leakage flow) re-enters the impeller.

Table 1 Flow rate of each section at Q=5.0L/min

Section	Type-A (L/min)	Type-B (L/min)
1-2	1.59	1.35
2-3	1.62	1.34
3-4	0.03	-0.38
4-5	0.50	0.15
5-6	1.82	1.51
6-7	1.22	0.95
7-1	0.33	0.06
Q_I	7.1	5.0

5. Radial Velocity

The distribution of a certain radial velocity and the velocity vector inside the pump at Q=5.0 L/min are shown in Fig.7 (a) for type-A and in Fig.7 (b) for type-B. Four sections are obtained from the mid-plane in between the blades as shown in the lower left corner of Fig.7. The flow patterns are shown with the thick arrows and marks. In Fig.7 (a) (α)-(δ) indicate the followings: (α) a forward current flowing at the center, (β) a backward current flowing along the volute wall, (γ) a backward current flowing back to the impeller, and (δ) a backward current flowing back to the gap. Figure 7 (c) is a close view of E in the A-A' section of (a). The positive value of the concentration map indicates the flow from the inlet to the volute (toward the left) and the negative value indicates the opposite.

In type-A of Fig.7 (a), the flow is symmetrical between the upper and lower sides in the direction of the height of the blade across the central line. In between the blades A-A' , B-B' and C-C', the forward current (α), which flows out of impeller, hits the volute wall and flows backward (β) toward the inlet along the upper and lower surfaces of the volute wall, forming two vortexes at the higher and lower sides of the volute. These vortexes are connected along the volute. When there is the gap, the backward current is divided into two flows: one re-enters the impeller (γ) and the other passes through the gap and flows backward toward the inlet (δ). Therefore, the amount of flow which directly flows back to the impeller decreases. Furthermore, it seems that (γ) does not flow in the inlet but flows out toward the volute along with the main flow. In D-D', which is located at the lower tongue, the backward current (γ) develops along the impeller wall and flows backward to the inlet while slowing down. As shown in Fig.7 (c), the backward current from the volute to the inlet develops in any areas in the gap. A similar flow is observed in the lower side of the gap as well. Such forward and backward currents inside the impeller and the backward current in the gap vary greatly according to the position of the blades. Therefore, it can be thought that the flow is extremely complex inside the pump in the three-dimensional view.

In type-B of Fig.7 (b), the forward and backward currents develop only inside the impeller as there is no gap. The flow inside the impeller is not symmetrical across the central line as in type-A, but both of the forward and backward currents flow asymmetrically, being deviated to the upper or lower wall. Especially in A-A', B-B' and C-C' sections, a clockwise or counterclockwise vortex appears around the tip of the impeller, and a forward or backward current develops along the vortex. Although detailed descriptions are not provided here, this vortex flows in and out of the impeller to the volute or shifts between the upper and lower sides with the impeller rotation. Hence, vortexes formed at the volute also become asymmetrical. This deviation of the flow could be the cause for the decreased pressure as shown in Fig.4. Considering all the above, it can be thought the gap in this pump induces development of the backward current not only inside the impeller but also in the gap. This prevents development of a deviated vortex inside the impeller, and as a consequence, the flow is rectified with the minimum loss of energy.

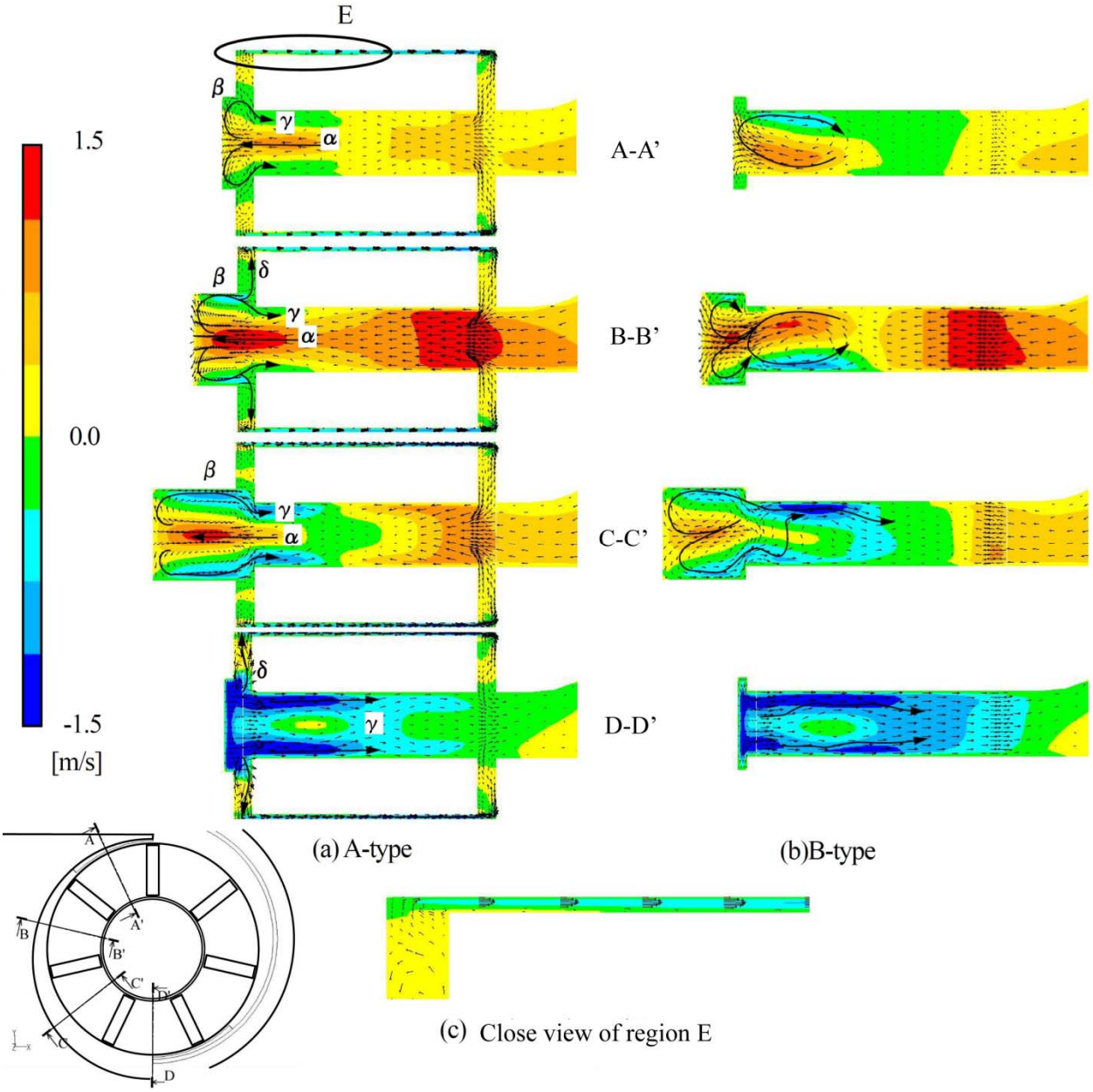

Fig. 7 Radial velocity of internal flow

6. Flow inside the Gap

The followings are described in Fig.8: (a) Radial velocity inside the upper gap at Q=5.0 L/min (the flow from inside to outside is defined positive), (b) pressure distribution, and (c) path lines. Each figure shows the result of computation at the central section in the direction of the height of the gap indicated as A-A' in Fig.8 (d).

According to Fig.8 (a), the radial velocity is negative for the entire circumference of the gap; the fluid flows in from the volute to the inlet, and the flow-in velocity is high especially around θ=110°-190° (area A) and 310°- 10° (area B). This is because the high pressure at the volute around the tongue as in Fig.6 (b) induces an increase of pressure in the areas A and B in the gap as in Fig.8 (b), resulting in high radial pressure gradient in these areas which makes it easier for the fluid to flows in. The flow paths in (c) show that the fluid in the gap flows (backward) to the inlet without causing stagnation while circulating in the same direction as the impeller rotation. Hence, it seems that an adequate "wash-out" effect has been achieved in prevention of thrombosis formation inside the narrow gap, which is one of the most significant elements of the blood pump. Similar tendency is observed at the different blade positions and also in the lower gap; further details are not provided here.

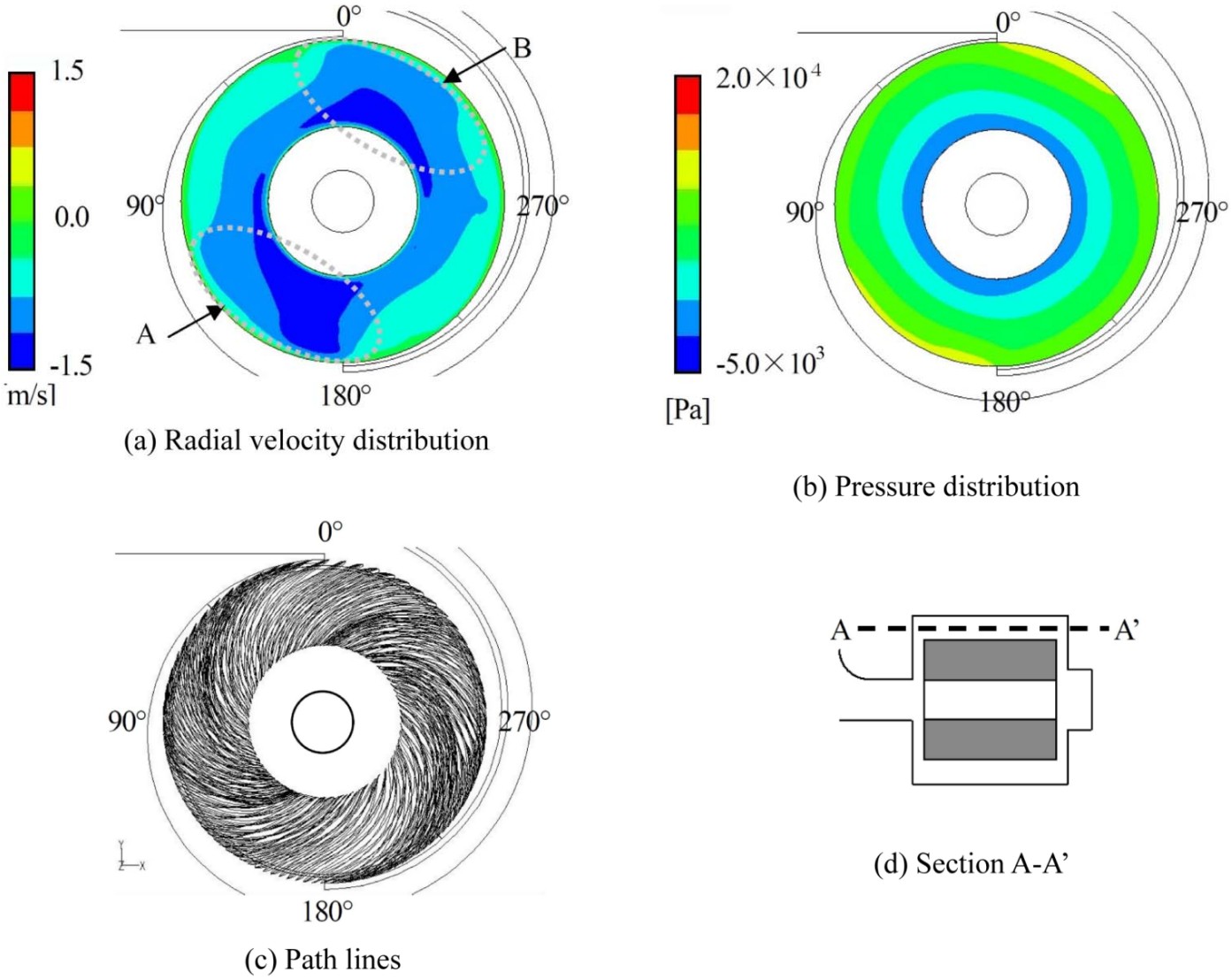

Fig. 8 Internal flow of gap section

7. Amount of the Gap Flow

The relationship between the amount of impeller outflow and the amount of gap flow is shown in Fig.9. The abscissa and ordinate indicate non-dimensional impeller outflow ϕ_I and non-dimensional gap flow $\phi_{L,}$ respectively. The gap flow ϕ_L is the amount of flow which passes all around the measuring surface of the upper and lower sides shown in Fig.9. Figure 10 presents (a) vorticity and (b) absolute value of vorticity of C-C' section (Fig.7) at non-dimensional flow coefficients ϕ=0.00 and 0.03. In Fig.10(a), vorticity is positive when it is counterclockwise and negative when it is clockwise. Figure 9 shows that there is hardly any difference between the upper and lower sides in the amount of gap flow. The value ϕ_L cannot be 0 within this computational range; there is always some leakage flow developing in the gap. Therefore, it can be concluded that an adequate wash-out effect is achieved in the gap from the small amount to the large amount of the flow. In Fig.10, when ϕ increases from 0.00 to 0.03, two vortexes, which appear symmetrically at the volute between the higher and lower sides, grow in size ($\alpha \rightarrow \alpha'$, $\beta \rightarrow \beta'$) and inhibit the flow going back to the inlet through the gap. As a result, it seems that ϕ_L decreases as ϕ_I increases as shown in Fig.9. When the output Q is 5.0 L/min, the amount of leakage flow Q_L is 2.1 L/min, and the amount of impeller outflow Q_I is 7.1 L/min (Q_L/Q_I=30%); the percentage of the amount of leakage is remarkably large compared to the ordinary large-sized pumps. Nevertheless, the generated pressure of type-A, where a leakage develops, is higher than in type-B, with no leakage, and it increases by about 10% in the low flow area (Fig.4). Therefore, it can be thought that the leakage flow counteracts against the tendency of pressure increase in the low flow area which is shown in the pump characteristics (Fig.4). In addition, Chua et al. [13] reported that Q_L/Q_I was 20% (Q_I=6.3 L/min, Q_L=1.3 L/min) at S_L =0.20 mm.

The relationship between the amount of non-dimensional impeller outflow ϕ_I and the total non-dimensional gap pressure ψ_{TL} is shown in Fig.11. The total gap pressure indicates the total pressure measured at each assessment surface in Fig.9. Within the

computational range, ψ_{TL} is similar between the upper and lower measurement surfaces. The value of ψ_{TL} decreases as ϕ_I increases, and approaches to 0 around ϕ_I =0.07. This indicates that the fluid which re-enters the impeller from the impeller inlet through the gap has been already energized by the impeller rotations. It can be thought that this condition, as a consequence, is a reason why the model with gap can achieve high pressure than the model without gap in terms of the characteristics of the pump in Fig.4.

On the basis of these findings, it can be concluded that the gap flow plays a crucial role in this pump, which is a low-specific velocity/low Reynolds number pump with a high percentage of leakage, although leakage is extremely low with a general industrial pump to the extent that it is not even an issue.

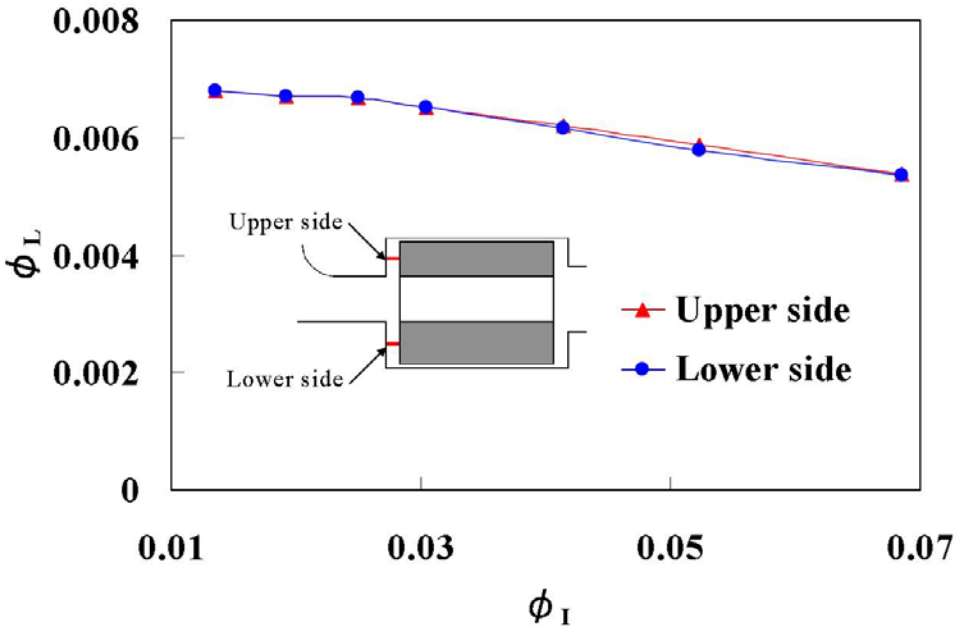

Fig. 9 Leakage flow rate

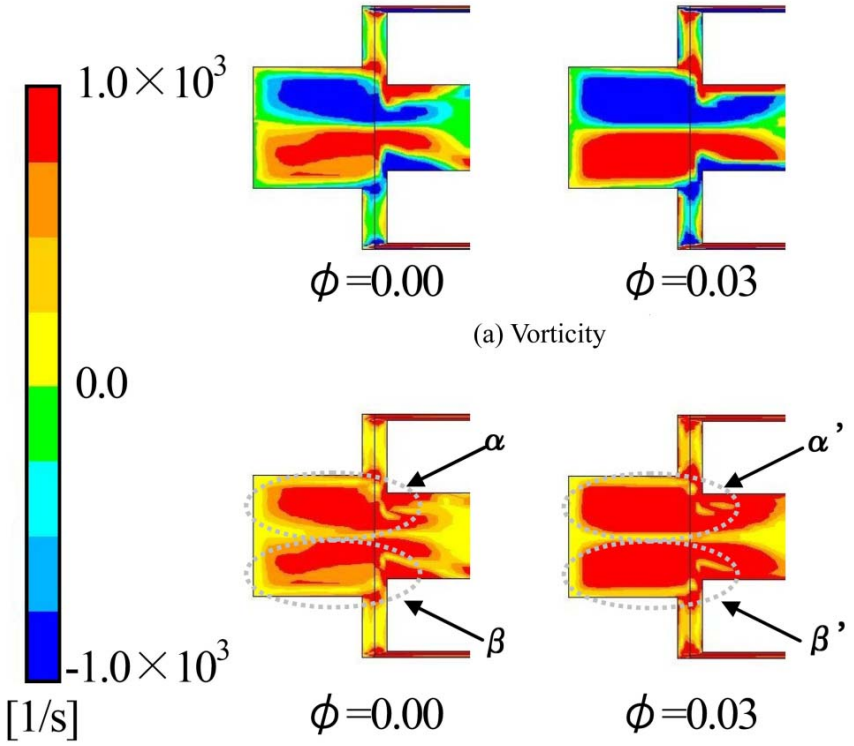

(a) Vorticity

(b) Absolute vorticity

Fig. 10 Vorticity distribution at C-C'

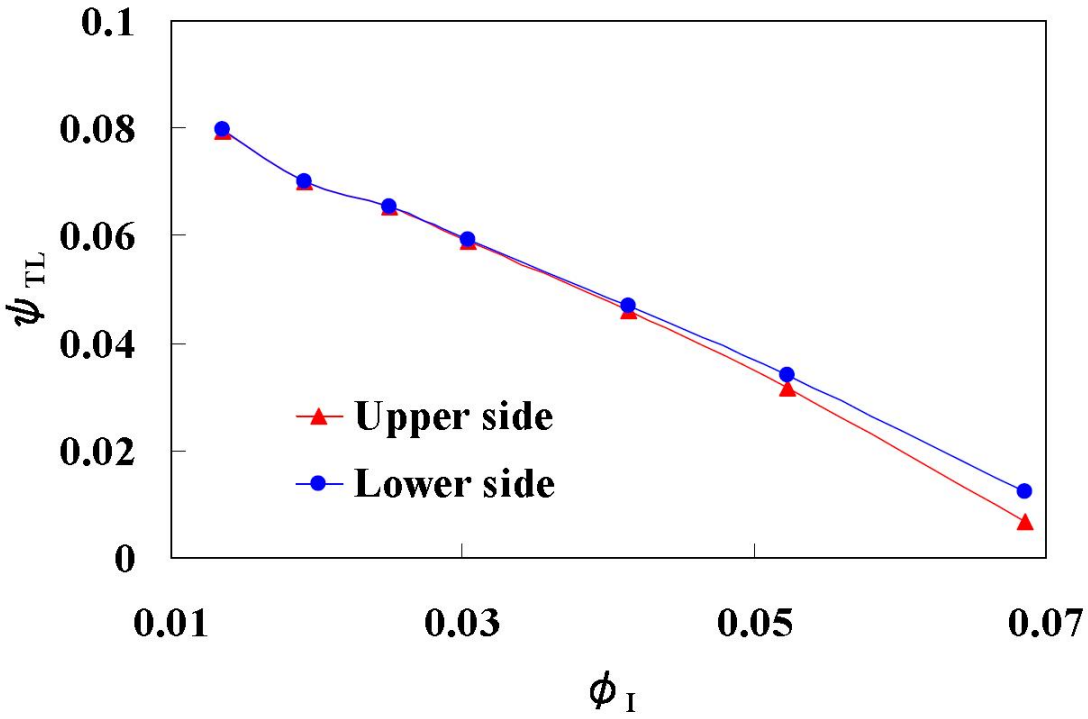

Fig. 11 Total pressure of leakage flow

8. Conclusions

In this study, comparisons were made between a model with which the gap between the impeller and casing of the magnetically suspended centrifugal blood pump was reproduced and another model without the gap. Using the thermal fluid analysis software numerical simulations were performed inside the pump to clarify the effect of the gap flow to the entire pump system. As a result, the followings have been revealed.

1. If there is a gap, the amount of the impeller flow increases as the fluid which comes back through the gap re-enters the impeller; hence, the backward current is reduced inside the impeller compared to that in the model without the gap, and as a consequence, the generated pressure increases.
2. If there is a gap, the impeller flow is rectified since vortexes, which are symmetrical between the upper and lower sides, develop inside the volute. Moreover, when the amount of flow increases, these vortexes grow in size and control the backward current inside the gap.
3. Within this computational range, the backward current (leakage flow) from the volute to the inlet always develops in the gap. Therefore, it can be thought that the wash-out effect, which is one of the most crucial elements in the blood pump, has been adequately achieved.

Acknowledgments

We very much appreciate Teruaki Akamatsu, Professor Emeritus of Kyoto University, for his various advices throughout this study.

Nomenclature

b	Height of blade [mm]	ν_B	Kinetic viscosity of blood [m^2/s]
n	Rotating speed [min^{-1}]	ρ_B	Density of blood [kg/m^3]
P	Pressure [mmHg]	ρ_G	Density of water solution of glycerol [kg/m^3]
P_{TL}	Total pressure at the gap [mmHg]	ϕ	Non-dimensional flow rate at the outlet: $\phi = Q / 2\pi r_2^2 b\omega$
Q	Discharge rate [L/min]		
Q_I	Discharge rate of impeller [L/min]	ϕ_I	Non-dimensional flow rate of impeller: $\phi = Q_I / 2\pi r_2^2 b\omega$
Q_L	Discharge rate at the gap [L/min]		
r_1	Impeller inner radius [mm]	ϕ_L	
r_2	Impeller outer radius [mm]		
Re	Mechanical Reynolds number $\mathrm{Re} = r_2^2\omega / \nu_B$	ψ	Non-dimensional flow rate at the gap:
S_L	Height of the gap [mm]		

Z_I	Number of the blade	ψ_{TL}	$\phi = Q_L / 2\pi r_2^2 b\omega$
μ_B	Viscosity of blood [Pa· s]		Non-dimensional pressure at
μ_G	Viscosity of water solution of glycerol [Pa· s]	ω	the outlet:
			$\psi = P / \rho(r_2\omega)^2$
			Non-dimensional total pressure at the gap:
			$\psi_{TL} = P_{TL} / \rho(r_2\omega)^2$
			Angular speed [rad/s]

References

[1] Kyo, S., et al., 2005, The Leading Edge Technology of Artificial Organ and Regeneration Medicine (in Japanese), Research Institute of advanced medical technology, Tokyo.

[2] Matsumiya, G., 2007, "Current state and the future of supplementary artificial heart treatment in our country (in Japanese)," Artificial Organs, Vol. 36, No. 3, pp. 244-247.

[3] Ono, M., 2007, "Artificial heart (clinical practice)," Artificial Organs, Vol. 36, No. 3, pp. 172-174.

[4] Akamatsu, T., 1994, "Centrifugal Blood Pump (in Japanese)," Turbomachinery, Vol. 22, No. 1, pp. 40-46.

[5] Akamatsu, T., 2001, "Study of the magnetically suspended centrifugal blood pump (in Japanese)," Turbomachinery, Vol. 29, No. 1, pp. 7-16.

[6] Akamatsu, T., et al., 1992, "Centrifugal Blood Pump with a Magnetically Suspended Impeller," Artificial Organs, Vol. 16, No. 3, pp. 305-308

[7] Tsukiya, T. and Akamatsu, T., 1995, "Development of the Centrifugal Blood Pump with Magnetically Suspended Impeller (in Japanese)," Transactions of JSME, 61-591, B, pp. 3913-3920.

[8] Terumo Heart Inc. Press Releases, http://www.terumo.co.jp/English/press/2007/005.html.

[9] Kurokawa, J., et al., 1990, "Characteristics of Spiral Pump at Low Specific Speed (in Japanese)," Turbomachinery, Vol. 18, No. 5, pp. 300-307.

[10] Kurokawa, J., et al., 1997, "Characteristics of Impeller at Very Low Specific Speed (in Japanese)," Turbomachinery, Vol. 25, No. 7, pp. 337-345.

[11] Matsui, J. et al., 2006, "Application of Circular Casing to the Centrifugal Pump of Low Specific Speed and the Internal Flow (in Japanese)," Turbo machine, Vol. 34, No. 8, pp. 463-470.

[12] Chua, L.P., et al., 2006, "Numerical Analysis of the Inner Flow Field of a Biocentrifugal Blood Pump," Artificial Organs, Vol. 30, No. 6, pp. 467-477.

[13] Chua, L.P., et al., 2005, "Computational Fluid Dynamics of Gap Flow in a Biocentirifugal Blood Pump," Artificial Organs, Vol. 29, No. 8, pp. 620-628.

[14] Ansys Inc., 2002, FLUENT 6.0 User's Guide.

[15] Ferziger, J. H., 2001, Computational Methods for Fluid Dynamics, Springer, New York.